Electronic Supplementary Material (ESI) for Nanoscale.

Purcell effect in active diamond nanoantennas. Supporting Information.

A.S. Zalogina,[†] R.S. Savelev,[†] E.V. Ushakova,[†] G.P. Zograf,[†] F.E. Komissarenko,[†] V.A. Milichko,[†] S.V. Makarov,[†] D.A. Zuev,[*,‡] and I.V. Shadrivov[*,‡,†]

ITMO University, St. Petersburg 197101, Russia, and Nonlinear Physics Center, Australian National University, Canberra ACT 2601, Australia

E-mail: d.zuev@metalab.ifmo.ru; ilya.shadrivov@anu.edu.au

Section 1. The average Purcell factor

In order to take into account presence of a large number of randomly oriented emitters which are uniformly distributed inside the diamond particle, we average the Purcell factor over the volume of the particle (assuming the uniform distribution of NV-centers inside the particle), i.e. we calculate the ratio of the averaged radiative decay rate of the emitter inside the particle to the corresponding rate in the bulk diamond. Due to broadband luminescence spectrum the corresponding spectral dependence of the Purcell factor is also normalized to the typical luminescence spectrum of NV-centers in spectral range 620-770 nm measured in our experiments. Overall the calculation formula for averaged Purcell factor $\overline{F_p}$ is the

*To whom correspondence should be addressed
†ITMO University, St. Petersburg 197101, Russia
‡Nonlinear Physics Center, Australian National University, Canberra ACT 2601, Australia

following:

$$\overline{F_p} = \frac{\int\limits_{\nu_{min}}^{\nu_{max}} \iiint\limits_{V} F_p(\mathbf{r},\nu)\, dV\, P_0(\nu)\, d\nu}{V \int\limits_{\nu_{min}}^{\nu_{max}} P_0(\nu)\, d\nu}, \tag{1}$$

where F_p is the Purcell factor that depends on the position of the emitter and the emission frequency, V is the volume of the particle, $P_0(\nu)$ is the typical luminescence intensity spectrum of NV-center as a function of frequency. In addition, since in the scattering spectra of sample particles we experimentally observed only low-Q resonances, we do not expect high values of the Purcell factor, that are predicted for lossless spherical particles with high-Q resonances. In order to better match the experimental results, we introduce small material losses and describe our nanoparticles with constant dielectric permittivity ($\varepsilon = 5.76 + 0.01i$). Losses were introduced only to avoid the appearance of the high-Q resonances, and therefore additional nonradiative decay rate caused by lossy medium was not taken into account. We note, that thorough averaging procedure requires to take into account the excitation field intensity distribution inside the nanoparticle, and the function under the integral (1) should be weighted with a function $W(\mathbf{r}) = \frac{|\mathbf{E}|^2}{|\mathbf{E}_0|^2}$. However, different resonances produce different field distribution, and due to non-spherical shape of the fabricated particles we cannot exactly determine the field distribution at the excitation wavelength of 532 nm in our experiments. Therefore, the shape of the particle can significantly affect the distribution of the excitation field and consequently the weight function $W(r)$. As a first approximation we consider $W(r)$ as a constant. Also, in these calculations the presence of a substrate is not taken into account. However, this can be justified, since the size of the nanoantennas is of the order of the emission wavelength, and the effect of a substrate on the emission properties of quantum emitters falls off exponentially with the distance from the substrate (with the strongest emission rate enhancement factors ${n_{glass}}^2$ and n_{glass} for perpendicular and parallel orientations of emitter, respectively). Therefore, the fraction of NV-centers affected by a glass substrate should be only of the order of a percent. We note that at the same time

the substrate will affect the frequency and the field distribution of the Mie modes in the nanodiamond, and in order to qualitatively correctly describe experiments, one would need to account for both the exact shape of the particles, as well as the substrate. The resulting average Purcell factor is shown in Fig. 1.

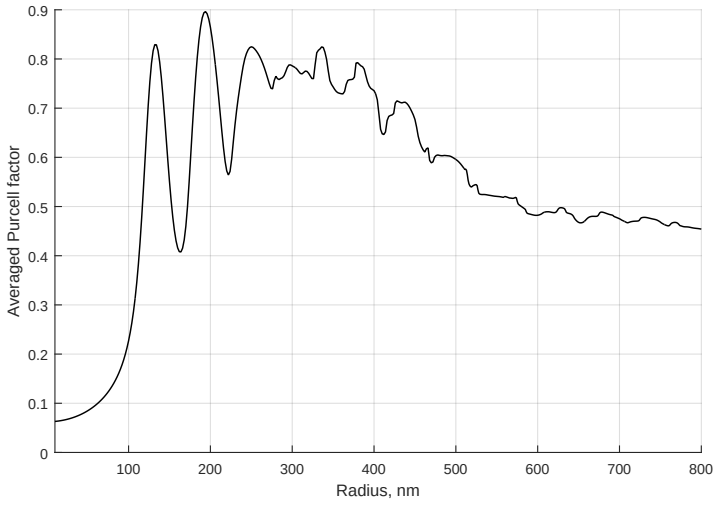

Figure 1: The dependence of the Purcell factor averaged over the volume of the spherical dielectric particle with permittivity $\varepsilon = 5.76 + 0.01i$ and over spectral range 620 nm-770 nm on its radius.

The ratio of average values of Purcell factor in resonant and nonresonant cases is 2 to 3,

which is in a good agreement with experimentally measured values.

Section 2. Nanodiamond fabrication.

Nanodiamonds are fabricated in Lebedev Physical Institute by plasma-enhanced chemical vapor deposition (PECVD) method on glass substrate .[1,2] PECVD process is used with a gas source of methane (CH4). To generate NV-centers nitrogen is implanted during the PECVD growth. The presence of NV-centers in nanodiamonds is evidenced by the zero phonon line in PL spectra of nanodiamonds (see Fig. 2).

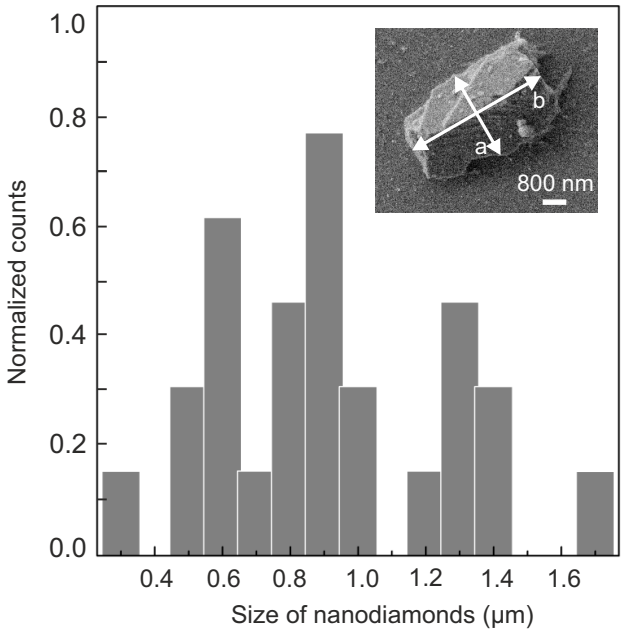

Figure 2: Size distribution histogram (statistics on 100 nanodiamonds) measured by SEM. Insert: SEM image of a nanodiamond.

Images of nanodiamonds are obtained using scanning electron microscope (SEM) Carl Zeiss Neon 40, and one example of the nanodiamond is shown in the inset in Fig. 2. The fabricated nanodiamonds are of irregular shapes with rough surfaces, and we measure the characteristic sizes as shown in the inset in Fig. 2. Statistical distribution of the nanodiamond sizes is shown in Fig. 2, showing median fabricated nanodiamond size of 900 nm.

Section 3. Raman Spectroscopy

In order to study the phase composition of nanoparticles, we measured Raman scattering spectra for individual nanodiamond particles using multifunctional setup Horiba LabRam HR. The sample is positioned by an XYZ-stage with 100 nm precision. The excitation source is HeNe laser with the wavelength of 632.8 nm. The exciting radiation is focused on the single nanodiamond with the objective (Mitutoyo M Plan APO VIS, 100, NA = 0.9) and the Raman scattered signal is collected by the same objective. The edge filter is used to filter the excitation light. Collected signal is send to the spectrometer and projected onto a thermoelectrically cooled charge-coupled device (CCD, AndorDU 420A-OE 325) with a 600 g mm^{-1} diffraction grating.

The analysis of nanodiamonds revealed that there are two types of nanoparticles: crystalline rough-surface and nearly spherical nanodiamonds. The Raman scattering of crystalline rough-surfaced nanodiamonds differ from the spherical one. The Raman spectra of rough-surfaced nanodiamonds are characterized by specific line at 1332 cm^{-1}. This line indicates strong coherent anti-Stokes Raman Scattering at the sp_3 vibrational resonance (C-C pair) of diamond and proves the presence of crystalline phase of diamond.[3]

The spherical nanodiamonds that have no zero-phonon line in photoluminescence spectrum are characterized by two broad asymmetric peaks: specific line of nanodiamonds at 1332 cm^{-1} and sp_2 vibrational resonances (C=C pairs) at 1590 cm^{-1} (Fig. 3). Such vibrational resonances are typical for surface bounds.[4] These nanoparticles could appear during nanodiamonds growth with unstable increase of methane concentration and a following formation of second nucleation and shell consisting of high-index crystal faces.[5]

By fitting the Raman spectrum with a superposition of four Gaussian trial functions of the form

$$y = y_0 + \frac{A}{\omega\sqrt{\pi/2}} exp \frac{-2(x - x_c)}{\omega^2}, \quad (2)$$

we reveal two overlapping peaks inside a broad peak at 1332 cm^{-1}. They are small and large

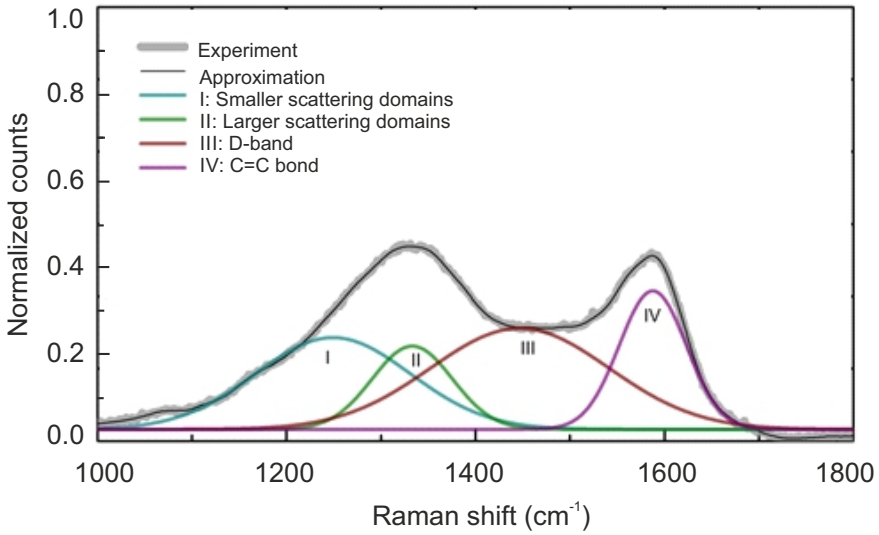

Figure 3: Raman spectra of spherical nanodiamond.

scattering domains at 1250 and 1340 cm^{-1}, respectively. Two other peaks are at 1410 and 1590 cm^{-1}, and they correspond to the carbon D- and G-band groups.

Section 4. Lifetime measurements

In order to measure the lifetime of the emitters, firstly, the experimentally obtained time-resolved luminescence curves were fitted by a biexponential function:

$$I(t) \;=\; A_0 + A_1 \exp(-t/\tau_1) + A_2 \exp(-t/\tau_2), \tag{3}$$

where A_1, A_2, τ_1, τ_2 and A_0 are the fitting amplitudes, decay times and background intensity, respectively. The average PL lifetime is calculated with the following equation:

$$\langle \tau \rangle \;= \sum_i A_i \tau_i^2 / \sum A_i \tau_i \tag{4}$$

Examples of fitting parameters normalized by $I(0)$ are presented in the table below.

number	A_0	A_1	t_1, ns	A_2	t_2, ns	$\langle\tau\rangle$, ns
8	0.0075	0.388	2.76	0.604	18.5	17.12
5	0.0075	0.284	2.35	0.708	17.3	16.50
12	0.0139	0.457	1.68	0.530	16.7	15.50
3	0.0001	0.386	3.62	0.614	15.8	14.26
7	0.0070	0.632	1.37	0.361	15.3	13.41
26	0.0040	0.477	0.87	0.519	13.2	12.49
1	0.0118	0.418	4.38	0.570	13.35	11.61
25	0.0028	0.776	0.35	0.221	11.1	10.03
40	0.0028	0.586	0.63	0.411	9.88	9.11
21	0.0023	0.863	0.57	0.134	11.3	8.67

Figure 4: Table 1. Examples of biexponential fitting parameters for 10 particles.

References

(1) Ivanova, A.; Ionin, A.; Khmelnitskii, R.; Kudryashov, S.; Levchenko, A.; Melnik, N.; Rudenko, A.; Saraeva, I.; Umanskaya, S.; Zayarny, D. *Laser Physics Letters* **2017**, *14*, 065902.

(2) Pham, M.; Pham, D.; Do, T.; Ivanova, A.; Ionin, A.; Kudryashov, S.; Levchenko, A.; Nguyen, L.; Nguyen, T.; Rudenko, A.; I.N.Saraeva, *Communications in Physics* **2017**, *27*, 37.

(3) Solin, S.; Ramdas, A. *Physical Review B* **1970**, *1*, 1687.

(4) Mochalin, V. N.; Shenderova, O.; Ho, D.; Gogotsi, Y. *Nature Nanotechnology* **2012**, *7*, 11–23.

(5) Feoktistov, N.; Grudinkin, S.; Golubev, V.; Baranov, M.; Bogdanov, K.; Kukushkin, S. *Physics of the Solid State* **2015**, *57*, 2184–2190.